

7/01/99

Energetic Particle Cross-Field Diffusion: Interaction with Magnetic Decreases (MDs)

Bruce T. Tsurutani¹, Gurbax S. Lakhina², Carlos Galvan¹, and Regina Sakurai¹

Jet Propulsion Laboratory¹
California Institute of Technology
4800 Oak Grove Drive
Pasadena, CA 91109

Indian Institute of Geomagnetism²
Colaba, Mumbai/Bombay, India

Abstract: Charged particle interactions with magnetic field magnitude changes lead to particle guiding center displacements and hence particle cross-field diffusion. We develop a diffusion model to apply to energetic ion interaction with magnetic field decreases detected by Ulysses at the polar regions of the heliosphere. The field decreases have minimum spatial scales sizes of 2-3 proton gyroradii and are typically bounded by tangential or rotational discontinuities. The distribution of the magnitudes of the field decrease is a continuum, with the smallest decrease being most frequent in occurrence. The largest decrease can be ~80% of the ambient field. The thickness distribution is also a continuum, and is shown to be independent of the field magnitude decrease. One specific example is used to illustrate rapid particle cross-field diffusion due to interaction with the magnetic decrease (MD) structures.

INTRODUCTION

The Ulysses spacecraft passed over the polar region (-80°) of the heliosphere for the first time in August 1994. The distance from the sun was 2.3 AU. Subsequent reports of the plasma and magnetic field measurements demonstrated that this region was dominated by a high-speed $\sim 750\text{-}800 \text{ km s}^{-1}$ solar wind emanating from a polar coronal hole (Phillips et al., 1994). It was also shown that these streams contain large amplitude ($\Delta\bar{B}/B_0 \sim 1$ to 2) noncompressive Alfvén waves (Tsurutani et al., 1994, 1995; Smith et al. 1995; Balogh et al. 1995; Goldstein et al., 1995).

The purpose of this paper is to demonstrate that there is another type of solar wind microstructure at high latitudes. The properties of the microstructures will be studied, and the effects on energetic charged particle propagation and transport will be developed.

RESULTS

Figure 1 is a plot of one month of magnetic field data centered at the highest latitude attained by Ulysses (-80°) at the south pole. The three magnetic field components are given in a SH coordinate system, where \hat{x} is radially outward from the sun, $\hat{y} = \hat{x} \times \hat{\Omega} / |\hat{x} \times \hat{\Omega}|$ where $\hat{\Omega}$ is the rotation axis of the sun, and \hat{z} forms the right-hand system. The field magnitude is given in the bottom panel.

The large amplitude fluctuations in the field components (top three panels) are primarily associated with Alfvén waves. The x, y, and z components have ± 1 nT variations in a ~ 1.2 nT magnetic field, so $\Delta \bar{B} / B_0 \sim 1$ to 2. The bottom panel shows the large magnetic field decreases that is the focus of this paper. The field occasionally decreases to 0.2 nT (the plots are one-minute averages) or $\Delta |B| / B_0 \sim 0.8$. For simplicity we call these phenomena magnetic decreases or MDs.

Figure 2 illustrates several of the MDs in higher time resolution. Panel a) shows a magnetic field magnitude decrease on September 7, 1994 from $\sim 0942:40$ to $0944:10$ UT. The field decreases from ~ 1.5 nT to as low as 0.2 nT. The field decrease is bounded by two sharp discontinuities. This is often the case. The discontinuities have been analyzed using the minimum variance method applied to the highest time resolution data (2s). The normal direction of the first discontinuity is oriented at 80° relative to the ambient magnetic field. The normal direction of the second discontinuity is 90° relative to the ambient field. The maximum field magnitude changes are from 1.25 nT to 0.8 nT for the first event and from 1.25 nT to 0.2 nT for the second event. $\Delta |B| / B_0 = 0.35$ and 0.8, respectively. The discontinuities are thus tangential in nature.

To attempt to place the magnetic decrease in context with the overall solar wind/field structures, we note that an Alfvén wave (see B_r component) is present from 0935:00 to 0953:30 UT. There is a fast field rotation from 0951:30 to ~0953:30 UT at the edge of the wave. There is a similar, but smaller field decrease at the field rotation. The latter feature is associated with the termination of the Alfvén wave. The magnetic decrease of primary interest was located near the center of the Alfvén wave.

Figure 2b illustrates another type of MD on September 11, 1994. The three field components given in minimum variance coordinates are noted to rotate smoothly throughout the whole MD structure from ~2151:40 UT to 2153 UT. The field is 1.4 nT prior to the decrease and 1.0 nT afterward. The magnetic field orientation changes significantly across the structure. The B_r component changes from ~ +1.0 nT to ~ -1.0 nT and B_n changes from -0.7 nT to +0.2 nT.

This MD is also bounded by sharp field magnitude decreases. The small discontinuity at 2151:40 UT has a normal component oriented $\sim 49^\circ$ relative to \bar{B}_0 . This appears to be a rotational discontinuity (RD) with a significant magnitude change (0.25 nT). The second discontinuity at ~2153 UT has a normal $\theta_{Bn} = 77^\circ$. For the latter event, the field magnitude changes from a 1.0 nT to 0.45 nT, or $\Delta|B|/B_0 = 0.55$. This is a tangential discontinuity (TD).

The third example is given in Figure 2c, from ~0652:40 to 0655:05 UT, September 3, 1994. The decrease is sharp at both edges of the MD. The normal angle θ_{Bn} is 89° for the first discontinuity and is 88° for the second. The field is 1.5 nT both prior to the MD and after the MD. The field decreases to 0.3 nT at the first discontinuity and to 0.45 nT at the second. Both discontinuities are clearly tangential in nature. Here the B_r component changes gradually across the MD. However the B_n component changes abruptly only at the second TD.

Figure 3 gives the distribution of the field decrease within MDs. 129 MDs with field magnitude decreases of $>20\%$ were examined. The field decrease is noted to be continuous with the smallest decreases the most common. The exponential fit is determined to be $129e^{-4 \Delta B/B_L}$.

The thicknesses of the MDs were calculated from the expression $\ell = V_{SW} \tau_{MD} \cos \theta_{nv}$, where V_{SW} is the measured solar wind velocity, τ_{MD} the "temporal thickness" of the MD and θ_{nv} the angle between the normal and the solar wind flow direction. The distribution of the thicknesses for the MDs in Figure 3 is given in Figure 4. Forty-nine percent of all discontinuities have thicknesses less than 4×10^4 km. The percent occurrence falls off with increasing thickness. In a 1.2 nT magnetic field, a 1 keV proton has a gyroradius of 6×10^2 km. The minimum thickness of the MDs is $2-3 r_p$ (not shown). Thus, half of the MDs have thicknesses between 2 and $7 r_p$.

Figure 5 shows the temporal thickness distributions for MDs with 20 - 30%, 30 - 40%, 40 - 50% and 60 - 100% decreases, respectively. The distributions are to first order the same. The MD thicknesses appear to be independent of the magnitude of the decrease.

The normals to the discontinuities were calculated using minimum variance analyses and the jumps in field magnitude were measured. The discontinuities are shown in Figure 6 in phase space. B_L is the larger field magnitude on either side of the discontinuity. Discontinuities with large relative magnitude changes and small normals (left-hand portion) are tangential discontinuities. The discontinuity normals are a continuum. A histogram is shown at the bottom of the Figure. The greatest number of discontinuities (49%) occur where the normals are the smallest, and the least number when the normals are the largest. The fit is $90e^{-3.6}$.

Particle - MD Interactions

We construct a particle diffusion model with the aid of some simplifying assumptions. These assumptions will be removed in further developments of the model.

Figure 7 illustrates the basic geometry of the interaction. The particle gyrates in a uniform magnetic field B_o (into the paper) with gyroradius “ r ”. The MD has a circular cross-section (simplification) of radius “ a ”. The field within the MD is in the same direction as the ambient magnetic field direction, but with reduced intensity. The “impact parameter”, the distance from the center of gyration to the center of the MD is “ d ”.

Figure 8 shows how the charged particle-MD interaction will move the particle guiding center perpendicular to the magnetic field. The particle has its guiding center at point O and the particle impacts the MD at point P_1 . Due to the abrupt change in the magnetic field strength from B_o to B_{MD} , the first adiabatic invariant is broken and the particle gyrocenter becomes point O' . The new gyroradius r' is equal to $r (B_o/B_{MD})$. The particle exits the MD at point P_2 with a new guiding center located at point O'' . Note that through this interaction the particle gyrocenter has moved from point O to point O'' . Below we will go through the geometry to determine the distance between points O and O'' . This value “ λ ” is a function of r , a and d .

To work on the exact expression of cross-field motion of the guiding center requires a few figures and geometrical calculations. Figure 9 shows Figure 8 with the impact parameter split into two parts, “ d_1 ”, and “ d_2 ”. With a few intermediate steps it can be shown that the half chord length “ ℓ ” is equal to

$$\ell = (a^2 - [a^2 + d^2 - r^2]/2d)^{1/2} \quad (1)$$

From simple geometry it can be shown that:

$$\lambda/2 = \ell' (r'-r)/r' \quad (2)$$

where ℓ' is the half-chord length with the particle gyrocenter at point O' . The expression for ℓ' can be given from examining Figure 8 and using an analogous expression from equation (1):

$$\ell' = (a^2 - [a^2 + d'^2 - r'^2]/2d')^{1/2} \quad (3)$$

where d' is the distance from O' to the center of the MD.

It can easily be shown (a number of steps are need) that the expression for d' is:

$$d' = ([\ell(r'-r)/r]^2 + [(r^2 - \ell^2)^{1/2}(r'-r)/r+d]^2)^{1/2} \quad (4)$$

The above four expressions give the value λ as a function of r , B_0 , B_{MD} , a and d .

In Figure 10, we illustrate the motion of the particle guiding center versus the normalized impact parameter, d/r . λ is given for three different scale sizes of the MD: $a/r = 0.05$, 0.1 and 0.5 . For all of the curves, $B_{MD}/B_0 = 0.5$. Note that the motion is finite and positive for $1-a/r < d/r < 1 + a/r$. For an impact parameter lying on the range $-1 - a/r < d/r < -1 + a/r$, the cross-field motion is in the negative direction with the same magnitudes.

Figure 11 gives the normalized cross-field motion λ/r as a function of normalized impact parameter, d/r , for various values of B_{MD}/B_0 (0.5 , 0.25 and 0.1). Clearly the largest motions are

associated with the case when the field magnitude change is the greatest ($B_{MD}/B_0 = 0.1$). All curves correspond to $a/r = 0.1$.

Acknowledgments. Portions of this research were performed at the Jet Propulsion Laboratory, California Institute of Technology, Pasadena, under contract with the National Aeronautics and Space Agency, Washington, DC. We wish to thank E. J. Smith for helpful scientific discussions.

REFERENCES

Balogh, A., E.J. Smith, B.T. Tsurutani, et al., The heliospheric magnetic field over the south polar region of the sun, *Science*, 268, 945, 1995.

Bavassano-Cattaneo, M.B., C. Basile, G. Morena and J.D. Richardson, Evolution of mirror structures in the magnetosheaths of Saturn from the bow shock to the magnetopause, *J. Geophys. Res.*, 101, 11961, 1998.

Goldstein, B.E., M. Neugebauer and E.J. Smith, Alfvén waves, alpha particles and pickup ions in the solar wind, *Geophys. Res. Lett.*, 22, 3389, 1995.

Hasegawa, A., Drift mirror instability in the magnetosphere, *Phys. Fluids*, 12, 1642, 1969.

McKenzie, J., F.W. I. Axford, and M. Banaszewicz, The fast solar wind, *Geophys. Res. Lett.*, 24, 2877, 1997.

Ho, C.M., B.T. Tsurutani, B.E. Goldstein, et al., Tangential discontinuities at high heliographic latitudes ($\sim 80^\circ$), *Geophys. Res. Lett.*, *22*, 3409, 1995.

Neugebauer, M., B.E. Goldstein, D.J. McComas, et al., Ulysses observations of microstreams in the solar wind from coronal holes, *J. Geophys. Res.*, *100*, 23389, 1995.

Phillips, J.L., A. Balogh, S.J. Bame, et al., Ulysses at 50° south: Constant immersion in the high-speed solar wind, *Geophys. Res. Lett.*, *21*, 1105, 1994.

Price, C.P., D.W. Swift and L.C. Lee, Numerical simulations of nonoscillatory mirror-mode waves at the Earth's magnetosheath, *J. Geophys. Res.*, *91*, 101, 1986.

Smith, E.J., A. Balogh, R.P. Lepping, et al., Ulysses observations of latitude gradients in the heliospheric magnetic fields, *Adv. Space Res.*, *16*, 165, 1995a.

Smith, E.J., A. Balogh, M. Neugebauer and D. McComas, Ulysses observations of Alfvén waves in the southern and northern solar hemispheres, *Geophys. Res. Lett.*, *22*, 3382, 1995b.

Tsurutani, B.T., C.M. Ho, E.J. Smith, et al., The relationship between interplanetary discontinuities and Alfvén waves; Ulysses observations, *Geophys. Res. Lett.*, *21*, 2267, 1994.

Tsurutani, B.T., E.J. Smith, C.M. Ho, et al., Interplanetary discontinuities and Alfvén waves. *Space Sci. Rev.*, *72*, 205, 1995.

Tsurutani, B.T., C.M. Ho, J.K. Arballo, et al., Interplanetary discontinuities and Alfvén waves at high heliographic latitudes: Ulysses, *J. Geophys. Res.*, *101*, 11027, 1996.

Winterhalter, D., M. Neugebauer, B.E. Goldstein, et al., Magnetic holes in the solar wind and their relation to mirror-mode structures, *Space Sci. Rev.*, Kluwer, Netherlands, 72, 201, 1995.

FIGURE CAPTIONS

Figure 1. The (south) polar magnetic field detected at 2.3 AU distance from the sun. The field is given in SH coordinates. The field magnitude plot illustrates the presence of frequent and large magnetic field magnitude decreases (MDs).

Figure 2. Three MDs examined in high time resolution. The MDs are often bounded by discontinuities with small normals (tangential discontinuities) and are typically 2 - 7 r_p wide.

Figure 3. Examination of all discontinuities with $\Delta|B|/B_L > 0.2$ bounding magnetic decreases in the interval Day 242 to 268, 1994. There are 131 events. The distribution is a continuum. There are fewer events with large B_N values.

Figure 4. The thickness distribution for the MD events in Figure 3.

Figure 5. The MD thickness distribution is independent of the magnitude of the field decrease.

Figure 6. The MD field decrease as a function of discontinuity normal.

Figure 7. Geometry of a particle gyromotion and a magnetic decrease.

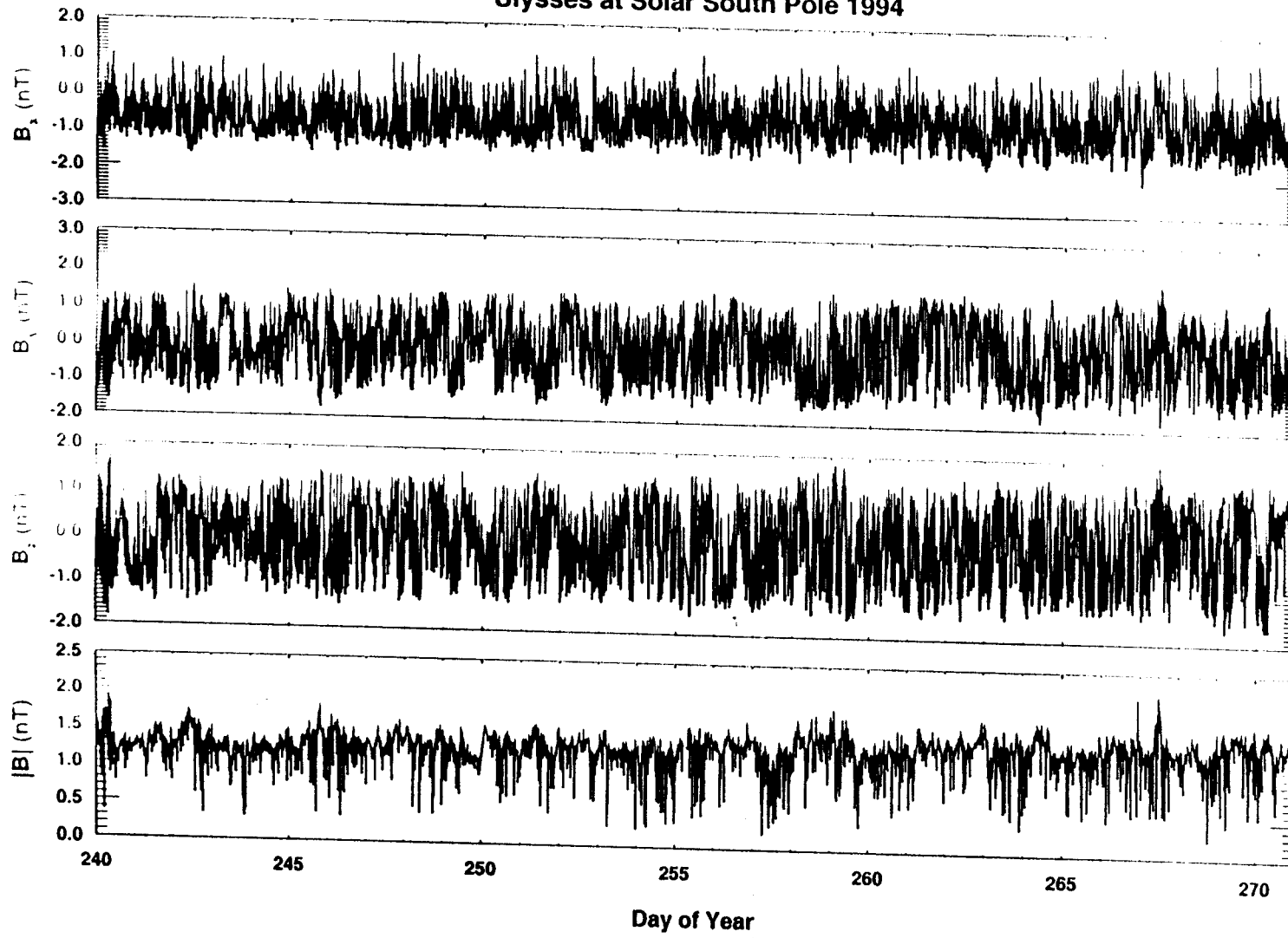
Figure 8. Schematic showing cross-field motion of the gyrocenter of a charged particle from the interaction with a MD.

Figure 9. Further geometry of a proton-MD interaction.

Figure 10. Cross-field motion (λ) as a function of impact parameter (d) and relative scale of MD radius (a) and ion gyroradius (r).

Figure 11. Same as Figure 10, but the various curves indicate different ratios of the magnetic field decrease in the MDs (B_{MD}) to the ambient field (B_0).

Ulysses at Solar South Pole 1994



September 3, 1994 (Day 246)

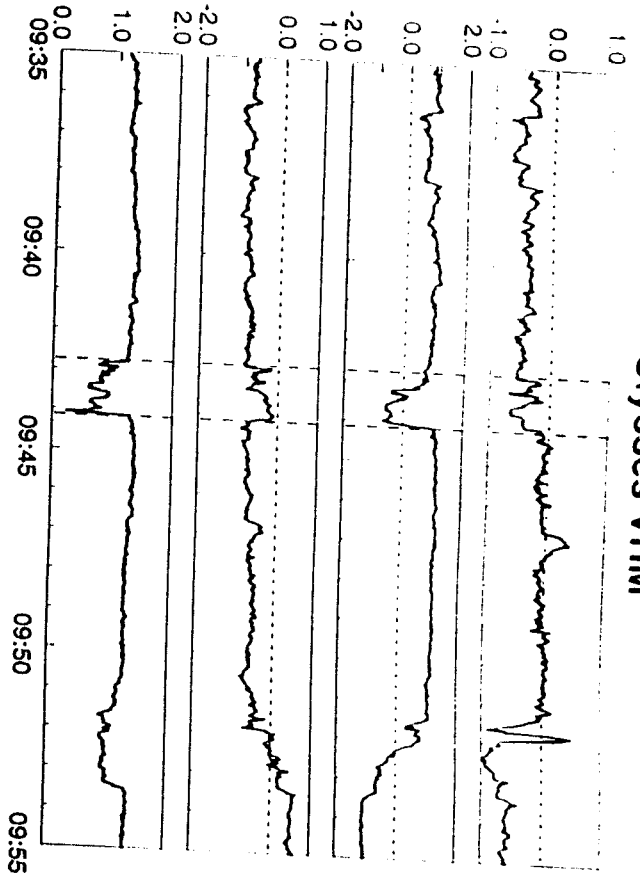
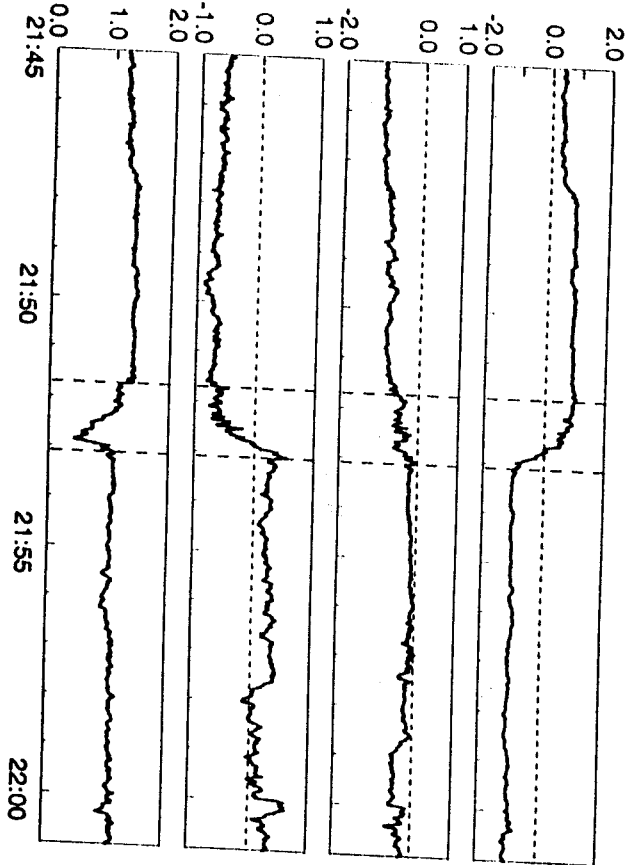
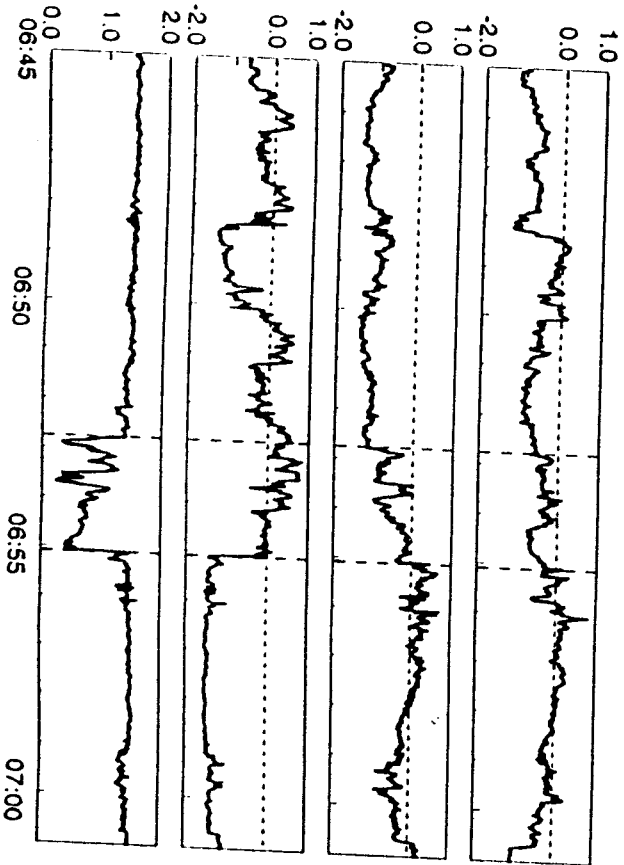
September 11, 1994 (Day 254)

September 7, 1994 (Day 250)

$|B|$ (nT) B_n (nT) B_t (nT) B_r (nT)

$|B|$ (nT) B_n (nT) B_t (nT) B_r (nT)

$|B|$ (nT) B_n (nT) B_t (nT) B_r (nT)



Ulysses VHM

Time, UT

Ulysses South Pole Days 242-268, 1994

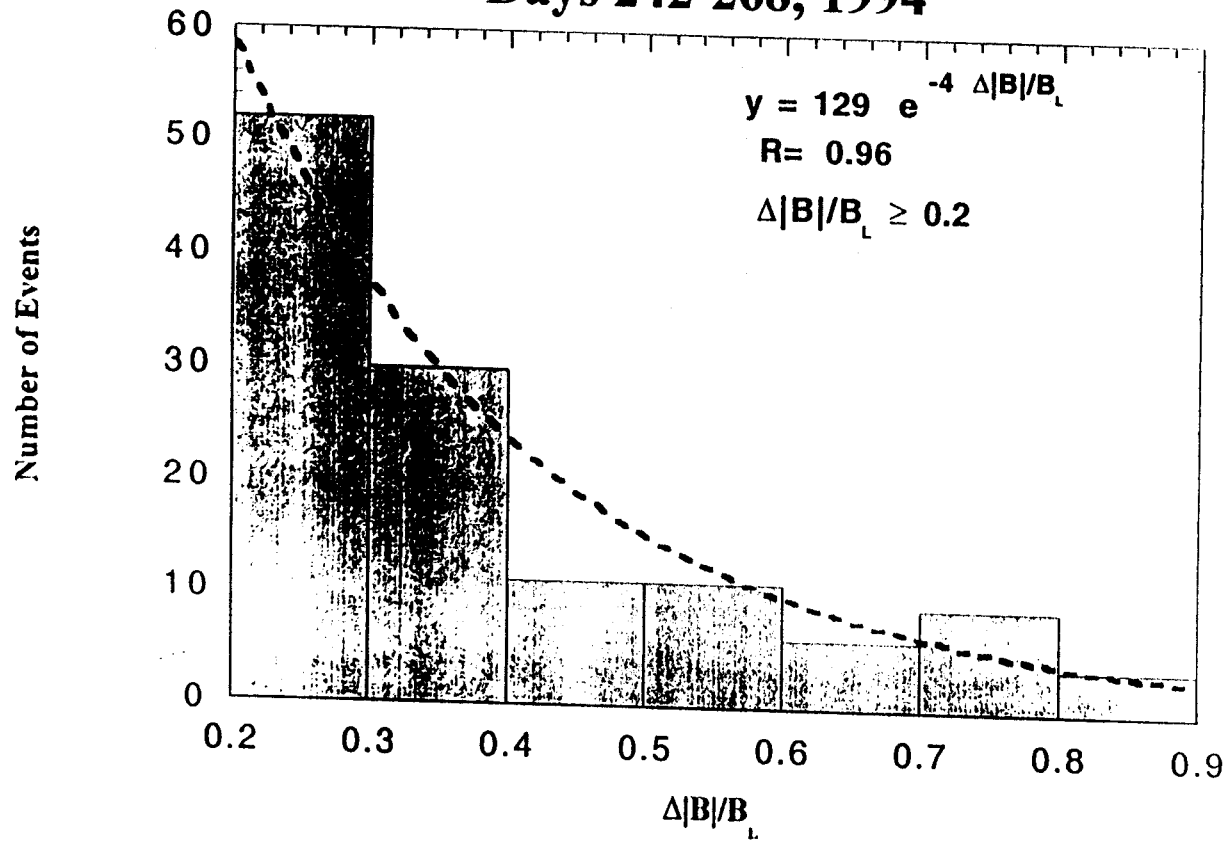


Fig 3

Ulysses South Pole

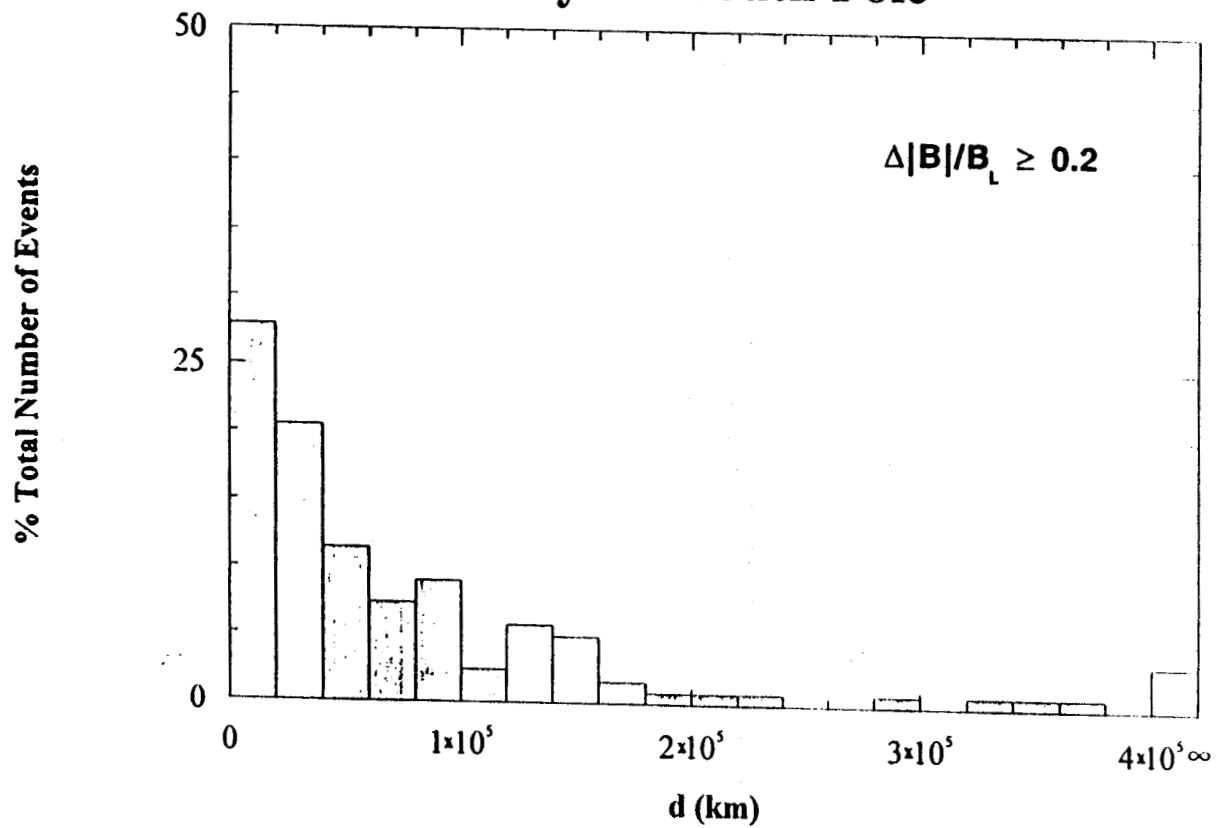


Fig 4

Ulysses South Pole Days 242-268, 1994

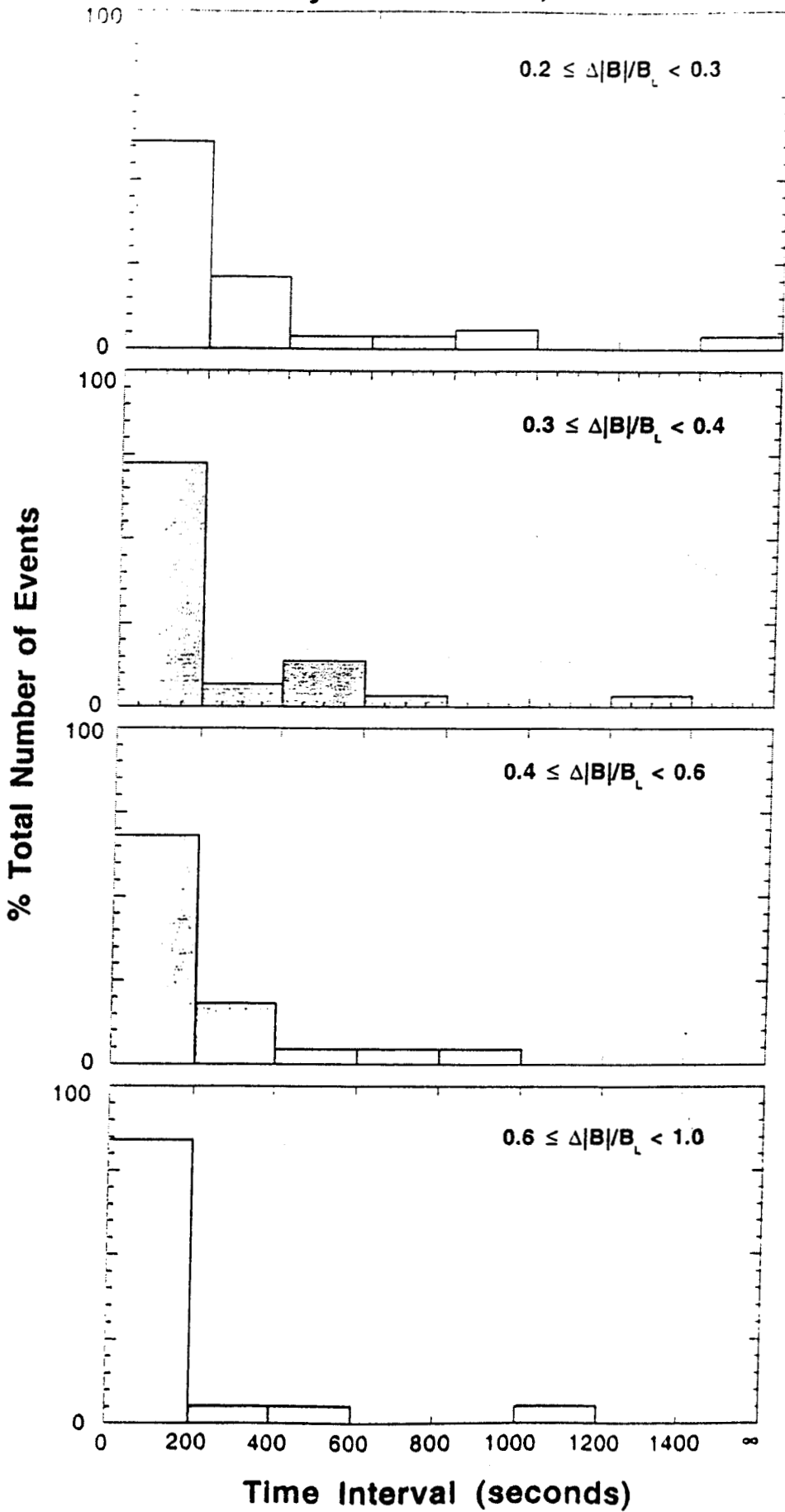
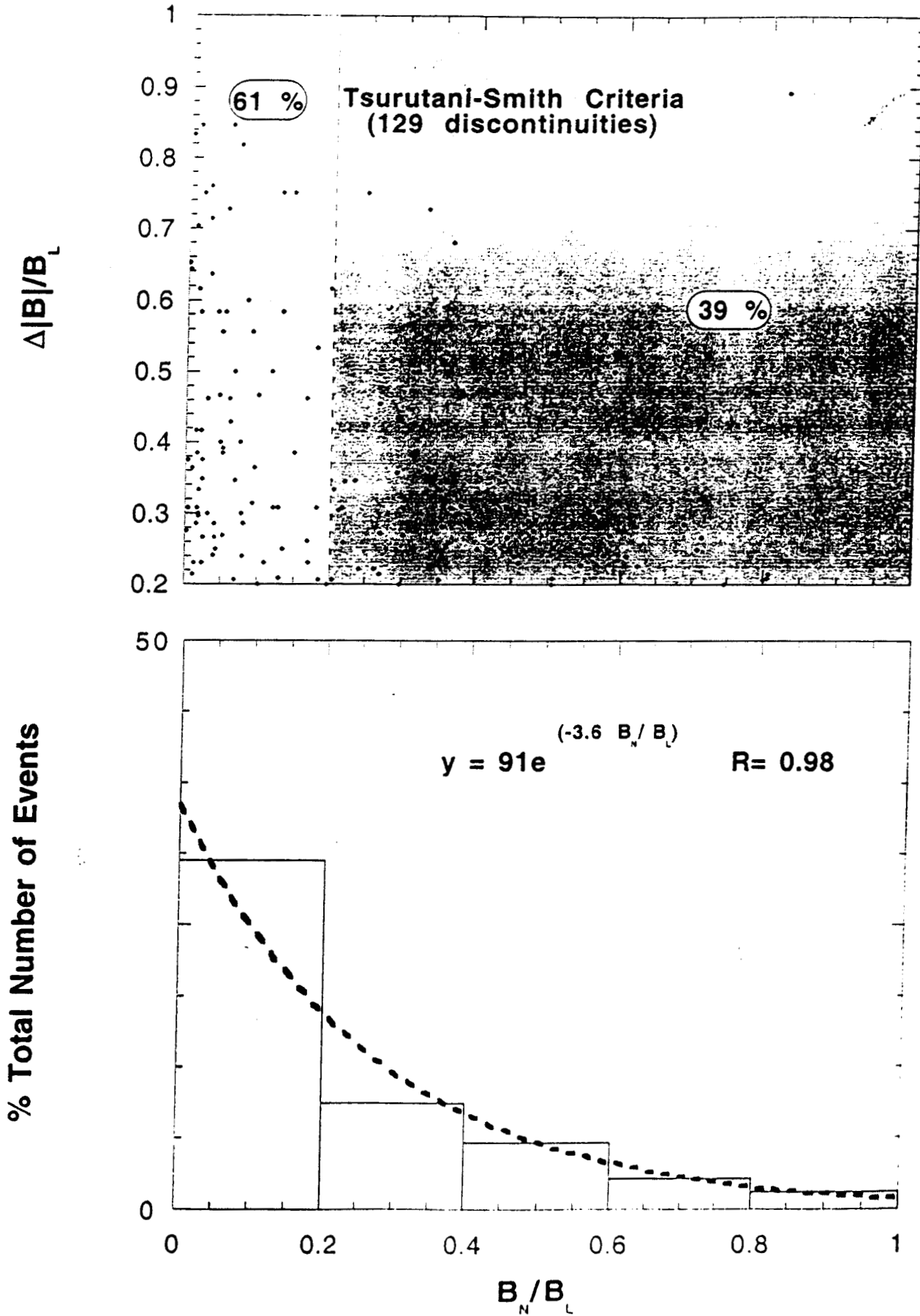
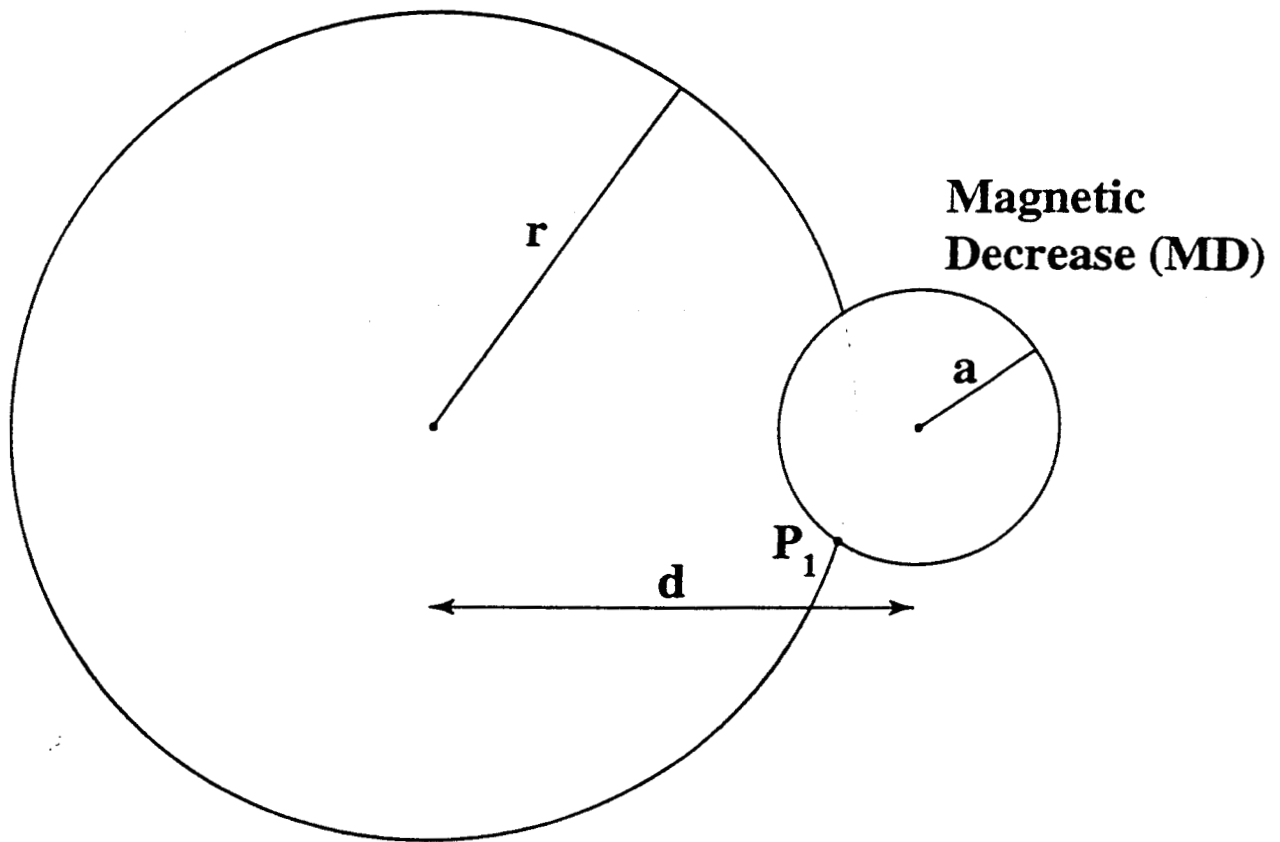


Fig 5

Ulysses South Pole Days 242-268 1994



Proton Gyromotion



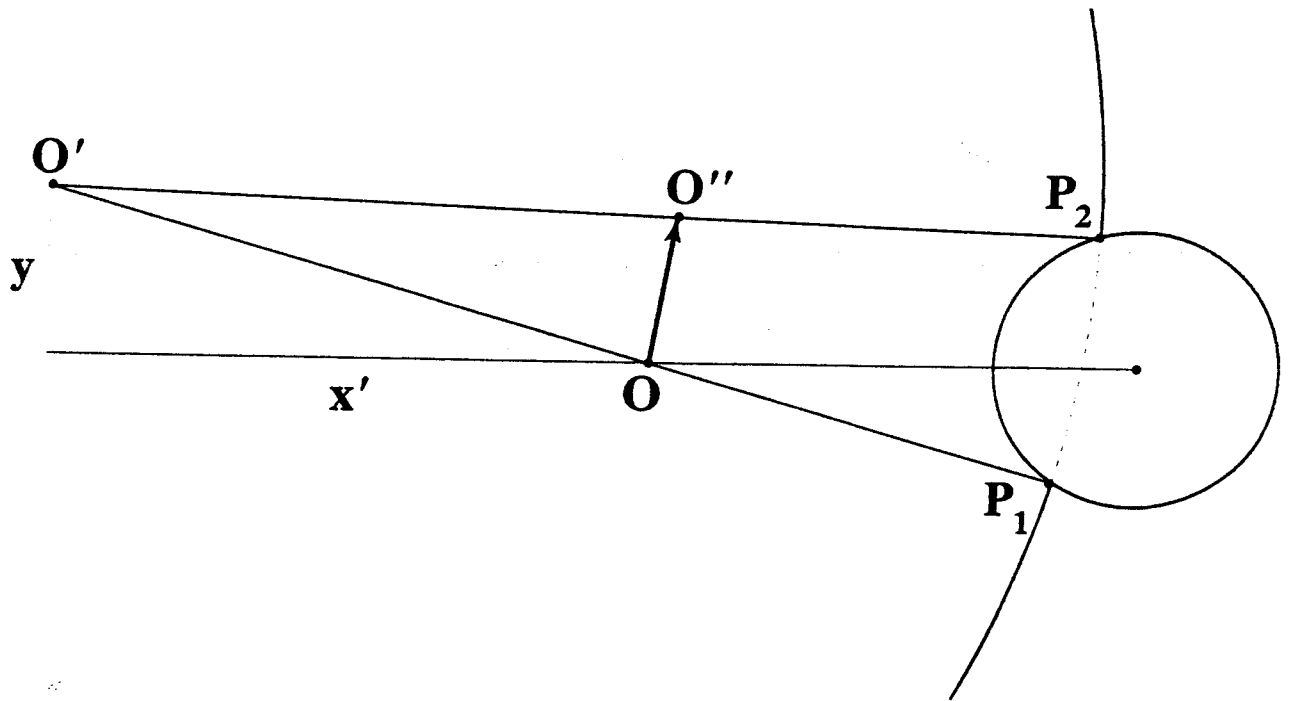
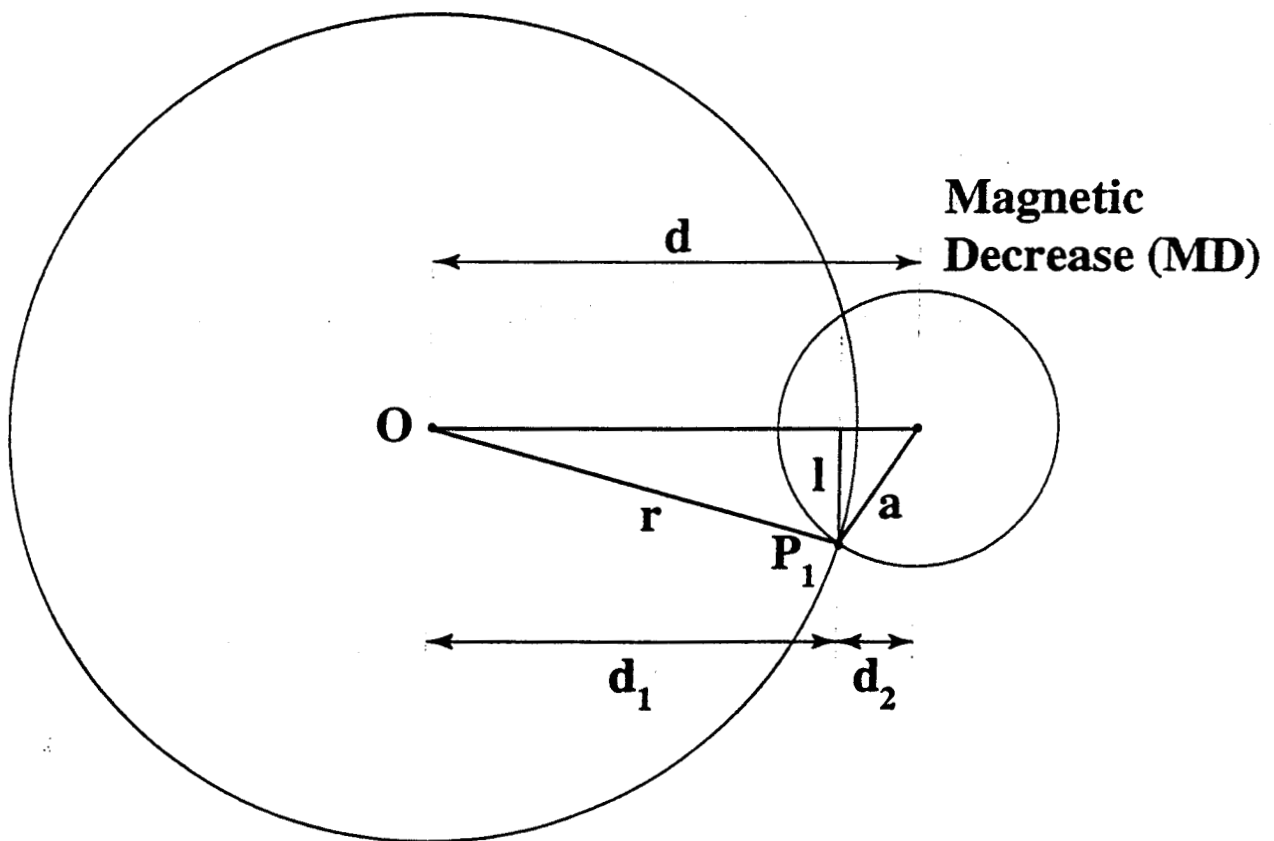
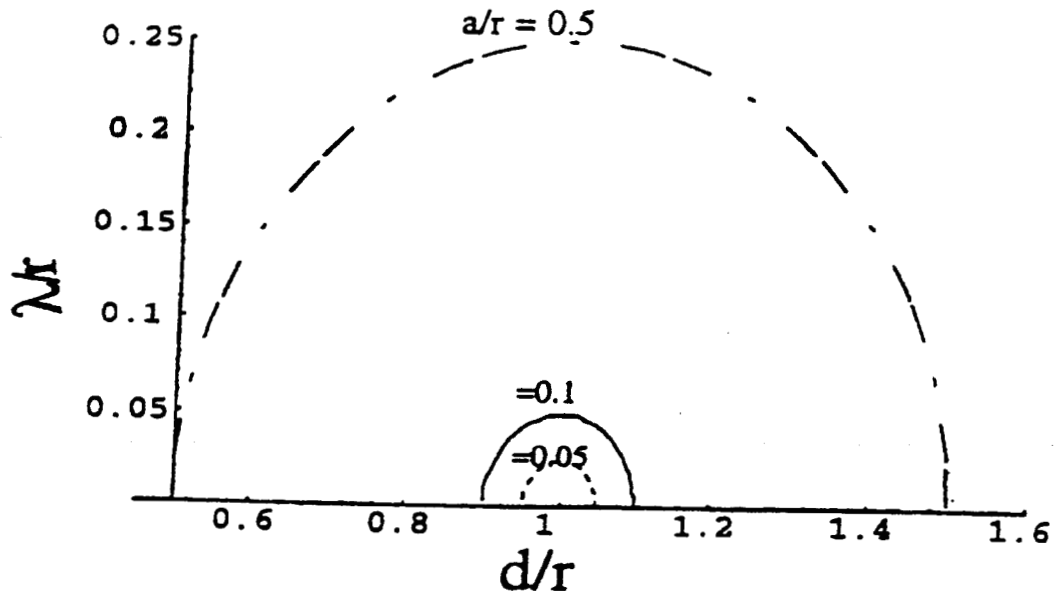


Fig. 8

Proton Gyromotion





17
 Figure 1: Variation of normalized cross-field motion of particle guiding center, λ/r , versus the normalized impact parameter, d/r , where r is the ion gyroradius., for three different scale sizes, a/r ($= 0.5, 0.1$, and 0.05), of the circular MD. Here, the ratio of the magnetic field inside the MD, B_{MD} , to that of the ambient field, B_0 , outside the MD is taken as $B_{MD}/B_0 = 0.5$. The cross-field diffusion of the guiding center is finite (and positive) for $(1-a/r) < d/r < (1+a/r)$ as shown here. For the impact parameter lying in the range $(-1-a/r) < d/r < (-1+a/r)$, the cross-field motion, λ/r , is in the negative direction, but the magnitudes are the same (not shown).

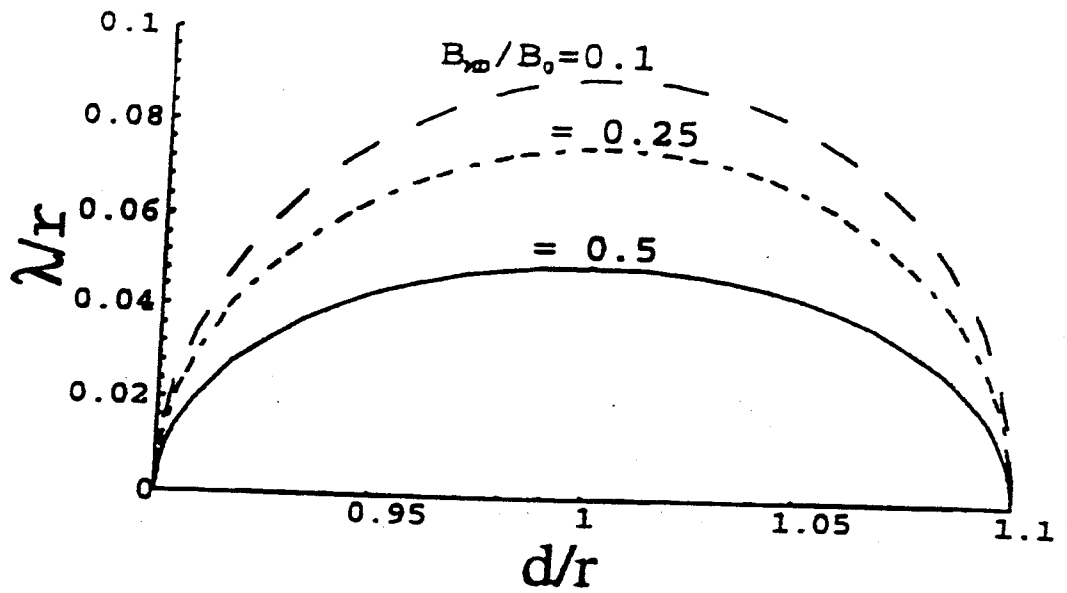


Figure 2: Variation of normalized cross-field motion of particle guiding center, λ/r , versus the normalized impact parameter, d/r , for different values of B_{MD}/B_0 ($=0.1, 0.25$, and 0.5) ratio. All the curves correspond to $a/r = 0.1$.